World Conference on Timber Engineering Oslo 2023

FULL-SCALE LATERAL TESTING AND MODELLING OF INDUSTRIALIZED TIMBER DIAPHRAGMS INCLUDING ONLY FRAMING AND NON-STRUCTURAL SHEATHING

Fernando Véliz[1], Xavier Estrella[2], Pablo Guindos[3]

ABSTRACT: Over the last decade, industrialized mid-rise light-frame timber buildings have gained popularity in Chile due to their structural, manufacturing, and environmental advantages. However, structural design aspects and industrialization prescriptions are not thoroughly addressed by national design codes, highlighting the need for developing standards to regulate industrialized earthquake-resistant timber systems. Therefore, this paper presents the outcomes of a large national project aimed at characterizing the lateral performance of a series of full-scale industrialized timber diaphragms employing Chilean materials. Eight 3.6x2.4 m specimens were tested under in-plane lateral load, considering different detailings such as sheathing, nailing, and framing. Besides, bare slabs (no sheathing) were also studied in the campaign. Strength results proved to be consistent with those proposed by international regulations, while chord tensions exceeded 30% of those obtained by principles of engineering mechanics. Additionally, it was found that adding gypsum boards over plywood does not considerably improve the global stiffness, although it considerably increased the in-plane strength. Finally, a finite-element numerical model was developed for the slabs studied in this campaign, proving to be capable of capturing the nonlinear behavior of the specimens under large lateral displacements.

KEYWORDS: Diaphragms, timber buildings, gypsum, I-joist, in-plane testing, numerical modeling

1 INTRODUCTION

Since the 1950s, low-rise wood-frame structures have considerably increased across seismic regions, with recent data [1] showing a bright future for multi-story timber buildings in the years to come. Nevertheless, the lower stiffness of timber structures can produce a detrimental impact on their performance. Such an issue shows the fundamental role of diaphragms in the performance of buildings under seismic loads [2] or wind action, influenced by the local diaphragm's behavior, either rigid or flexible [3] as classified by [4]. Several experimental campaigns [5-10] have proven that both the shear capacity and stiffness of diaphragms are primarily dependent on the sheathing-to-framing connection [6].

Even though a large amount of research has been oriented to the traditional light-frame diaphragms, there is still a lack of studies focused on I-Joist diaphragms. For example, concerns about the validity of applying the same design provisions to conventional and I-joist diaphragms [11], have led designers to challenge such design methods, mainly due to the potential splitting of I-joist flanges, which was not addressed in those codes. Such concerns were partially addressed through I-joist diaphragm tests, such as those conducted by Weyerhaeuser, whose results have been reported by [12]. Among other outcomes, the researchers found that a lower shear strength improvement on I-joist diaphragms was reached when replacing 6d nails with 10d nails (+16% strength), compared to that improvement reached using sawn-lumber joists diaphragms and the same nails (+70% strength), attributable to flange splitting. Furthermore, other investigations such as the one conducted by [13], which considered eight 7.3x7.3 m I-joist diaphragms, proved that wooden I-joist diaphragms meet the design values specified in the Special Design Provisions for Wind and Seismic SDPWS standard [14], whose parameters were originally calibrated based on sawn lumber tests.

The new tendency of building higher timber buildings has raised concerns about the fire resistance of these structures. Such a concern is usually solved using gypsum boards. The structural contribution of gypsum panels has been experimentally assessed, however, putting the focus on gypsum sheathing over shear walls [15-17]. Some studies have tested gypsum sheathing attached to ceilings [18], which was supposed to improve their in-plane strength within the linear range. Such lack of data led authors [19-20] to study the contribution of gypsum sheathing in diaphragms. Then, an experimental campaign shown in [18] assessed the contribution of gypsum over ten full-scale (3.7 x 4.9 m) plywood roof

[1] Fernando Véliz, Centro Nacional de Excelencia para la Industria de la Madera (CENAMAD), Pontificia Universidad Católica de Chile, fdveliz@uc.cl
[2] Xavier Estrella, Ecole Polytechnique Federale de Laussane, Switzerland, edisson.estrellaarcos@epfl.ch
[3] Pablo Guindos, Centro Nacional de Excelencia para la Industria de la Madera (CENAMAD), Pontificia Universidad Católica de Chile, pguindos@ing.puc.cl

https://doi.org/10.52202/069179-0447

diaphragms, including both pitched and flat specimens. Such investigation focused on determining if the diaphragm strength or stiffness was increased by adding a 12 mm thick gypsum board, evaluating also the impact of employing different roof pitches. Tests confirmed that the increase in apparent stiffness for flat roofs is negligible; by contrast, gypsum increased the apparent stiffness of gable roofs by an average of 32% and hip roofs by 21%.

An important lack of houses has been noted in Chile the last decade, estimating a need of 650.000 units [21]. The main alternative chosen by the Housing Ministry to afford this lack is associated with industrialized construction, which can reduce manpower, time and overall cost, while better quality houses are obtained in contrast to using the traditional method [22]. Nowadays, guidelines such as the SDPWS [14] standard used to design timber structures in Chile, since no design recommendations are available in local regulations [21] to date. Therefore, the present investigation aims at contributing with scientific data for the inclusion and regulation of industrialized timber diaphragms in the Chilean code [21], including both experimental and numerical information of different typologies through an experimental campaign.

2 EXPERIMENTAL STUDY

As previously mentioned, this research is mainly focused in providing both experimental and numerical information for timber diaphragms, considering different typologies, including I-Joist framing as well as sawn-lumber framing, and non-structural ceiling panels over the diaphragms, so these contributions can be experimentally measured in terms of strength and stiffness. To address these issues, a set of 8 industrialized full-scale diaphragms 3.6 x 2.4 m were tested as part of the investigation presented in this paper according to ASTM E-455 loading protocol [23], considering a third-point load condition, and the results were used to validate the numerical models presented in a subsequent section of this document. The so-called numerical model was based on M-CASHEW software [24] and following the modeling guidelines proposed by [25].

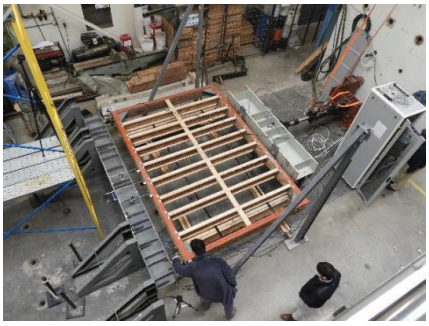

Figure 1: *Layout of the lateral testing of the specimens.*

2.1 DIAPHRAGM SPECIMENS

Different parameters were considered such as using sawn lumber joists as well as I-joists, assessing the contribution of gypsum panels over the structural sheathing and including different type of fasteners. Four diaphragms were constructed using 41 x 185 mm (2'' x 8'') sawn-lumber framing, graded as a C24 Chilean Radiata Pine [26]. The other four specimens were built using LSL as chord-and-end beams, while 241 mm deep LPI18 I-joists were used as interior beams, attached to LSL beams with ITS2.56/9.5 Hangers, and spaced at 407 mm on center.

Sawn-lumber (SL) specimens' chords were attached using Simpson Strong-Tie HRS416Z Straps, thus allowing to install strain gauges more easily, to experimentally obtain the chord tension. Every specimen was attached in their corners with four steel angles – attached by means of 8 shear bolts, 22 mm in diameter and 150 mm in length – to prevent early failures at the chord-to-end beam joint.

The first specimen of each configuration (sawn-lumber and I-joist), consisted of a bare slab, to measure the timber frame's stiffness, and then compared to the stiffness of the sheathed specimens. The sawn-lumber bare specimen was tested to failure, while, the I-joist specimen was tested only up to a design load, aiming at re-using it.

The second specimen of each configuration was designed with the same framing as the bare specimens. Nevertheless, these specimens were reinforced with an 11.1 mm thick APA rated OSB panel as sheathing on one side of the framing. The sawn-lumber diaphragm employed 2.9 x 65 mm smooth shank nails, spaced at 100 mm on center for the edge nailing, and 150 mm at adjoining panel edges parallel to the load direction. The I-joist diaphragms' panels were attached to the framing using 2.5 x 50 mm ring shank nails, spaced at 65 mm on center in the edge of the panels, and 100 mm at the adjoining panel edges parallel to the load direction. In all cases, field nailing was set to 300 mm on center . The third specimen of each configuration was similar to the second one, however, in this configuration the diaphragms were sheathed with a 15.1 mm thick plywood panel instead of 11.1 mm OSB, employing the same nails and nailing patterns for each case.

Finally, the fourth specimen of each configuration was equivalent to the third one, however 15 mm thickness gypsum boards were attached with of 8 x 75 mm drywall screws over the plywood sheathing, to evaluate the contribution of the non-structural sheathings. A brief list of the specimens is presented in Table 1.

Table 1: *Labeling and description of test specimens.*

Label	Nail spacing (mm)		Panel	t	Nail
	Edge	Joint*		mm	(mm)
SL – BARE	-	-	-	-	-
SL – OSB	100	150	OSB	11.1	2.9x65
SL – PLY	100	150	Ply	15.1	2.9x65
SL - PLY/GWB	100 (300)	150 (300)	Ply (Gyp)	15.1 (15)	2.9x65 (8x75)
IJ – BARE	-	-	-	-	-
IJ – OSB	65	100	OSB	11.1	2.5x50
IJ – PLY	65	100	Ply	15.1	2.5x50
IJ - PLY/GWB	65 (300)	100 (300)	Ply (Gyp)	15.1 (15)	2.5x50 (8x75)

https://doi.org/10.52202/069179-0447

(*) Adjoining panel edge parallel to load direction.

2.2 TEST SET-UP

A reinforced-concrete reaction wall and a strong floor were used to carry out the tests. As shown in Figure 2, a H500x500x246 mm steel beam was connected to a 250 kN capacity hydraulic actuator, to distribute the load to the specimens in two points, by means of load-transfer plates, as shown in Figure 1. Rollers were placed under the diaphragms to braced them, avoiding out of plane displacements. Load cells were attached to a 4000 mm long W10x48 reaction beam and placed near to the corners of the unloaded chord of each diaphragm. Four angle brackets supported the 4 meters long reaction beam and were also anchored to the strong floor using post-tensioned steel bars, thus ensuring that the friction between steel plates and strong floor was greater than applied load by the hydraulic actuator.

The adopted set-up was designed to position the specimens in a flat manner, parallel to the strong floor, and placed over steel bars to allow the diaphragm to move under in-plane loads. Each test was instrumented with eleven linear variable displacement transducers (LVDT), to measure different displacements, such as those in the unloaded chord beam, between sheathing panels, displacement in the angle brackets, among others. A system connected to a PC was used to collect the data.

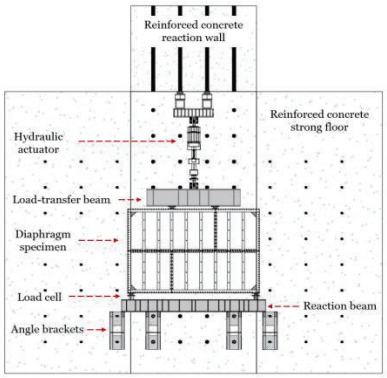

Figure 2: *Plan view of test set-up. Taken from [27].*

2.3 LOADING PROTOCOL

Tests were carried out based on the guidelines provided by the ASTM E455 standard [23]. SL – OSB and SL – PLY specimens were tested according to a loading protocol (force-controlled) based on [9], as shown in Figure 3. Both tests were performed considering a design load of 50 kN, however, to evaluate the stiffness degradation at low/high load levels, the SL – OSB specimen started the loading protocol at the fifth cycle, and loaded to the failure at the end. Conversely, the SL – PLY specimen started the loading protocol at the very first cycle and loaded to the failure after the fourth 1x design load cycles. Stiffness results can be found in [27].

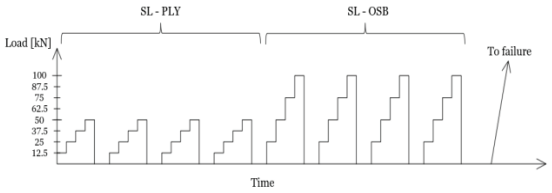

Figure 3: *Loading protocol for SL-PLY and SL-OSB specimens.*

The rest of the specimens were tested under a monotonic loading protocol, all of them displacement-controlled, with a displacement rate of 5 mm per minute. Load was stopped when the peak load dropped by approximately 20%.

3 NUMERICAL MODELING

Numerical models are a valuable tool for researchers when studying the nonlinear response of structures since they provide the means to overcome the physical and resource limitations of lab testing. However, numerical models also require a validation process against real specimens to measure their reliability level, precision, and prove that they meet the minimum requirements for structural engineering, beings this latter especially relevant when unconventional systems or solutions are studied. Therefore, this section presents a nonlinear numerical model for the timber diaphragms tested as part of this research project, validates its results against the test data presented in previous sections, and carries out additional analyses to better understand the nonlinear response of industrialized timber diaphragms. The numerical model has been developed employing the M-CASHEW software built by [24] and following the modeling guidelines proposed by [25].

Timber beams were represented using Euler-Bernoulli frame elements (elastic response) that have 3 degrees-of-freedom at each node. An elasticity modulus E = 11.4 GPa was considered for the sawn lumber model, based on the experimental results reported by [25]. Also, an elasticity modulus of 11.5 GPa were employed for I-joist beams according to [28], and 9.3 GPa for LSL, according to values declared by the manufacturer. Besides, the frame elements employed a corotational approach in the numerical formulation. Nailed connections were modeled employing zero-length spring elements with 3 degrees-of-freedom per node. The so-called MSTEW model proposed by [29] for nonlinear timber connections was employed in the X and Y direction, whereas a zero-stiffness element was considered for rotations. It should be noted that the elements used for the directions X and Y employed the true-oriented approach developed by [24] with the aim of avoiding overestimated values for the diaphragm's capacity and stiffness, as has been found by prior investigations [29,30]. The governing parameters for the MSTEW model were computed by nonlinear minimization techniques from the test data on nailed connections similar to [31].

The sheathing panels were modeled by means of shear rectangular elements with 5 degrees-of-freedom: one for rigid-body rotation, two for in-plane shear deformation, and two for rigid-body translation. Note that panels' rigid behavior consider the bearing between them. Based on the experimental data from [25], a shear modulus G = 1.3 GPa was used when modeling the OSB panels, and G = 0.5 GPa when modeling plywood panels, according to Table C4.2.3A of SDPWS [14]. When conducting analyses with the model, a displacement-controlled approach was employed along with a norm displacement increment test as convergence criteria. Besides, up to 20 iterations were conducted at each load step and the residual tolerance was set as 1e-6 kN. Full details on the modeling approach can be found in [25] and [27].

4 RESULTS AND DISCUSSION

4.1 FAILURE MODE

The diaphragms presented failure modes related to fasteners, as usually shown in the literature [5-13]. All specimens failed due to pull out of the nails in the edges of the panels (Figure 4a, 4c), crushing of OSB panels, cutting of drywall screws (Figure 4d) and a non-expected failure in the loaded chord of SL-PLY specimen (Figure 4b). The frame structure appeared to remain undamaged, particularly in the unloaded chord beam. Steel angles in each specimen prevented undesired end-beam to chord-beam joint failure, allowing them to exhibit typical ductile failure modes.

The smooth shank nail used in SL diaphragms led these specimens to show failure modes associated to pull out of the nails, due to their low friction resistance. In case of SL-PLY/GWB, no shear cracking was seen over the gypsum boards. Conversely, the main failure was due to the cutting of drywall screws and pulling out of the nails attaching the edges of the plywood underneath, as shown in Figure 4d.

Most of the investigations on I-joist diaphragms have considered nail spacings not closer than 102 mm, and employing 10d sheathing nails [11-13], which increased the probability of flanges to split. Thus, this paper attempted to reduce nail spacing, reducing the nail diameter at the same time, minimizing as much as possible the probability of splitting without decreasing shear capacity. As shown in SL specimens, failure modes on IJ specimens were also due to pull out of nails and crushing of panels by nails head. IJ-OSB, IJ-PLY and IJ-PLY/GWB specimens showed ductile failure modes as previously mentioned, although IJ-PLY also presented brittle failures located at blocking, like those reported in [13]. As well as in SL-PLY/GWB, the failure mode of IJ-PLY/GWB was partially due to the cutting of drywall screws, added to local gypsum failures and detachment, as reported in [31]. No cracking of global gypsum panels was reported, as shown in Figure 4e. Further results are available in [27].

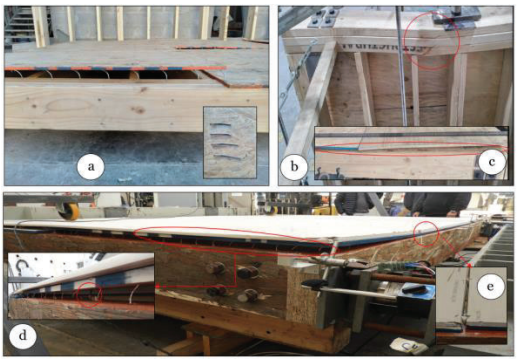

Figure 4: *Typical failure modes of diaphragm specimens.*

4.2 FORCE-DISPLACEMENT RESPONSE

The monotonic and envelope curves are plotted in Figure 5. The y-axis located in the right shows unit shear capacity, which is the peak capacity divided into 2 and then divided into the width of the diaphragm. Initially, the monotonic response was approximately linear up to drift values (midspan displacement divided into half mid-span length) of about 0.2-0.5% for SL specimens, and up to 0.6% for IJ specimens [27]. Bare specimens appeared to behave virtually elastic according to Figure 5.

Beyond the mentioned drifts, the structural response turned to be highly non-linear, mainly due to the local deformation of nails. A summary of the main results is listed in Table 2, which includes peak capacity on each test (F_0), elastic stiffness (K_0), yielding load (F_y), yielding displacement (δ_y) according to ASTM E2126 [33] and ductility ratio (μ), which was obtained as δ_u / δ_y. Note that ultimate displacement δ_u was omitted from Table 2 due to space constraints.

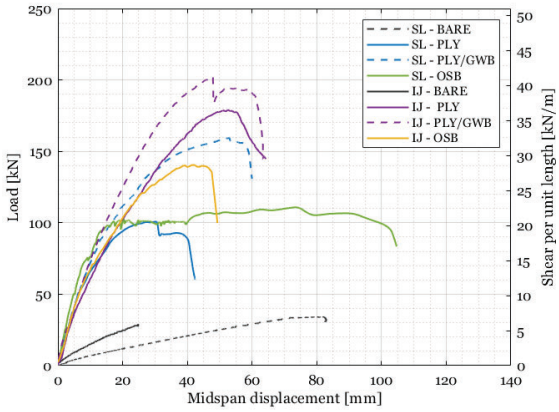

Figure 5: *Force versus mid-span displacement response.*

https://doi.org/10.52202/069179-0447

Table 2: *Summary of experimental results. Adapted from [27].*

Tested Diaphragm	F_0 kN	K_0 kN/mm	F_y kN	δ_y mm	μ -
SL – BARE	33	0.5	-	-	-
SL – OSB*	110	11.4	104	9.8	10.6
SL – PLY*	100	9.3	92	11.2	3.71
SL -PLY/GWB	160	7.5	145	19.2	3.11
IJ – BARE	-	1	-	-	-
IJ – OSB	141	7.6	125	17	2.85
IJ – PLY	179	5.5	156	26.8	2.36
IJ – PLY/GWB	203	6.6	182	25.2	2.5

(*) Envelope curves were used to obtain the parameters presented.

4.3 AXIAL CHORD TENSION EQUATION CHECKING

The most common way for modeling diaphragms analytically, and to estimate their chord tensions comes from principles of engineering, where the diaphragm is assumed as a deep and thin beam, thus the sheathing panels act as the web, supporting the shear, and the chords act as flanges, supporting all the axial tension, which is usually estimated as M/W, where M is the flexural moment diagram along the chord, and W is the width of the diaphragm. Thus, this research included two specimens (SL-OSB and SL-PLY) to assess how well this assumption fits with the experimental results. Both specimens were instrumented at the unloaded chord with one strain-gauge each, as shown in Figure 6. To consider the contribution of both straps, the axial load measured in each strain-gauge was. The comparison was evaluated at the shear allowable design of each specimen: for SL-OSB (4 kN/m), the experimental axial chord tension indicated 7.4 kN, with a theoretical tension of 5 kN, thus showing a 48% of percentage difference. For SL-PLY (shear limit of 4.5 kN/m), the experimental measurement recorded a value of 6.6 kN, in contrast to 5.5 kN from the theoretical estimation, showing a 20% of percentage difference. Such percentage differences confirmed thw well-functioning of such an assumption, and in particular the M/W equation, even though experimental results appear to be slightly higher. These underestimations may be attributable to the axial load duplication, since axial loads at the instrumented strap were probably higher than those at the non-instrumented strap, due to the eccentricity with respect to the shear resistant zone, i.e., the sheathing panel. Further research needs to be carried out on this topic.

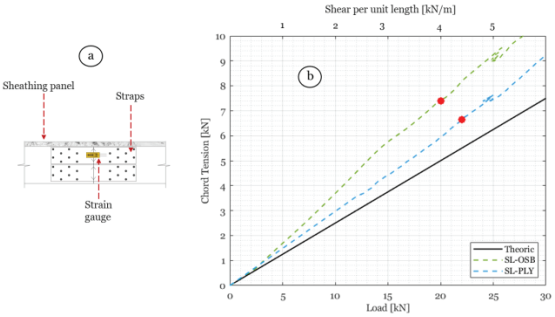

Figure 6: *Chord tension measurements versus theorical M/W estimation: (a) shows the location of strain gauge and in (b) is shown the measurements up to the starred allowable design limit.*

4.4 DESIGN IMPLICATIONS

This section compares the experimental results with the estimations of strength and stiffness provided by SDPWS [14]. This section is intended to evaluate how well code provisions adjust with the experimental results reported in the present investigation. Even though SDPWS standard is only applicable to diaphragms uniformly nailed, and just with one type of sheathing per specimen, PLY/GWB specimens were also Ied in this section, but not deeply discussed.

4.4.1 Strength

The nail sizes and sheathing panels used in this research were chosen for being commonly used in the Chilean industry, however, they were not coincident with North 5merican configurations, then they were not applicable to meet SDPWS [14] available unit shear capacities. Thus, two different methods to obtain unit shear capacities (v_{SDPWS}) were employed in the present research. The first consisted of choosing the more similar configuration from Table 4.2A of the SDPWS [14] standard. Thus, considering 6d common nails (2.87 mm in diameter) and 9.5 mm (⅜ in) sheathing panels, nominal unit shear capacities were taken from 4 – 6 in nailing pattern (785 plf) and 2.5 – 4 in nailing patterns (1175 plf) to compare with SL specimens and IJ specimens, respectively. In contrast, the second method consisted in estimating allowable unit shear capacities for each specimen by means of Johansen's theory [34], as explained in [9]. Following these approaches, experimental and theoretical shear capacities for each specimen were shown in Table 3. Experimental unit shear capacities for SL specimens were between 78-96% larger than those proposed in SDPWS [14], while for IJ specimens the experimental to SDPWS [14] nominal contrast were between 68-114%. Allowable unit shear capacities were obtained by dividing experimental and SDPWS nominal values by 2.8, as suggested in [14]. Conversely, Tissell & Elliot [9] method was chosen to properly estimate allowable unit shear capacity for each specimen, allowing to take into account the accurate variables for every specimen, such as nail size, sheathing thickness, among others. Such a method allowed to calculate the allowable unit shear capacity of

each specimen through their Johansen's yielding mode [34], multiplied by the nails separation. Table 3 shows in its lasts two columns the allowable unit shear capacity derived from [9] method. As it can be highlighted from Table 3, conventional SL specimens reached experimental-allowable unit shear capacities between 61-100% higher than those proposed via [9] method, while conventional IJ specimens exhibited experimental-allowable unit shear capacities between 144-172% higher than those proposed via [9] method. On the other hand, since both experimental and SDPWS nominal results were divided into 2.8, percentage variance are the same as those presented above.

Table 3: *Nominal and allowable unit shear capacity.*

Test	Nominal		Allowable (ASD)		
	v_{exp} kN/m (plf)	v_{SDPWS} plf	v_{exp} plf	v_{SDPWS} plf	$v_{T\&E}$ kN/m (plf)
SL – OSB	22.5 (1540)	785	550	280	4 (275)
SL – PLY	20.5 (1400)	785	500	280	4.5 (310)
SL – PLY/GWB	32.8 (2250)	-	805	-	-
IJ – OSB	28.9 (1980)	1175	710	420	4.2 (290)
IJ – PLY	36.7 (2515)	1175	900	420	4.8 (330)
IJ – PLY/GWB	41.6 (2850)	-	1020	-	-

* T&E: Tissell & Elliot [9].

4.4.2 Stiffness and deflections

The stiffness of a uniformly nailed diaphragms may be indirectly calculated from SDPWS Eq (4.2-1), which is usually employed to calculate the mid-span displacement within linear range. This equation is relevant since it allows to predict whether the diaphragms will behave rigidly or flexibly in contrast to the lateral force resisting system underneath, according to principles such as those published in [4]. The mid-span displacement is calculated as follows:

$$\delta = \frac{5vL^3}{8EAW} + \frac{vL}{4G_v t_v} + 0.188Le_n + \frac{\sum x\Delta_c}{2W} \quad (1a)$$

$$\delta = \frac{5vL^3}{8EAW} + \frac{0.25vL}{1000G_a} + \frac{\sum x\Delta_c}{2W} \quad (1b)$$

Equation (1a) includes bending, panel shear deformation, nail slip, and chord splices slip, while Eq. (1b) eases the use of the first equation by combining both shear flexibilities, generating an apparent diaphragm shear stiffness G_a, which is a function of nail slip in the linear range. Under the same logic as in section 4.4.1, since no SDPWS [14] configurations are exactly coincident with those carried on in this research, G_a values were calibrated with the monotonic and cyclic (envelopes) sheathing-to-framing tests presented in [27], which were used to determine the nail slip e_n in equation C4.2.3-3 in SDPWS [14], and presented here as Equation (2):

$$G_a = \frac{1.4v_{ASD}}{\frac{1.4v_{ASD}}{G_v t_v} + 0.75e_n} \quad (2)$$

where $G_v t_v$ correspond to shear stiffness of wood structural panels. Due to the lack of precisely information, values from Table C4.2.3A from SDPWS [14] were taken, where 14.6 kN/mm (83500 lb/in) and 7.5 kN/mm (43000 lb/in) were considered for 11.1 mm thickness OSB and 15.1 mm thickness plywood, respectively. G_a values were tabulated in Table 4, which also shows all the parameters considered for each of the 4 conventional specimens tested to be used in Equation (1b).

Table 4: *Mid-span displacement comparison at allowable design levels.*

Tested Specimen	SL – OSB	SL – PLY	IJ – OSB	IJ – PLY
L (mm)	3663	3663	3663	3663
L (ft)	12	12	12	12
E (Gpa)	11.4	11.4	9.3	9.3
E (psi × 10^6)	1.65	1.65	1.35	1.35
A_{chord} (in^2)	35.3	35.3	33.2	33.2
W (mm)	2443	2443	2443	2443
W (ft)	8	8	8	8
x (mm)	1831	1831	-	-
x (ft)	6	6	-	-
Δ_c (in)	0.003	0.003	-	-
G_a (kips/in)	7	5	11.5	6.5
v_{ASD} (lb/ft)	275	310	290	330
δ_{SDPWS} (in)	0.12	0.19	0.07	0.15
δ_{SDPWS} (mm)	3.07	4.81	1.94	3.89
δ_{exp} (mm)	1.69	2.56	2.59	3.22
$\delta_{SDPWS}/\delta_{exp}$	1.81	1.87	0.75	1.21

Load-displacement curves were calculated for each specimen presented in Table 4 and were plotted against the corresponding experimental results. As shown in Figure 7, each conventional specimen (uniformly nailed and with one sheathing) was plotted until the corresponding allowable shear limit, defined in Table 3 and Table 4 in the y-axis, while the x-axis was limited to 0.27% drift, equivalent to 5 mm of mid-span displacement. Note that most of specimens behaved

https://doi.org/10.52202/069179-0447

slightly stiffer than their corresponding SDPWS [14] prediction, being the only exception the specimen IJ – OSB, whose percentage difference was about 25%, probably attributable to a poor nailing process. These outcomes may provide a first overview of how conservative this equation is for estimating mid-span displacements inside the linear range for Chilean industrialized diaphragms. Although not a fair comparison, non-conventional specimens which included gypsum boards were included in Figure 7 with the purpose of showing the difference in contrast with conventional systems.

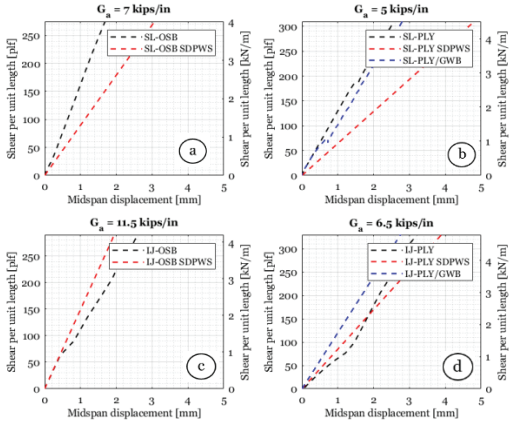

Figure 7: *Measured and calculated mid-span displacement curves for allowable design levels: (a) SL-OSB specimen, (b) SL-PLY and SL-PLY/GWB, (c) IJ-OSB specimen, and (d) IJ-PLY and IJ-PLY/GWB specimens. Adapted from [27].*

4.5 NUMERICAL MODELING

This section had the purpose of confirm the well-functioning of the M-CASHEW [24] software at modeling diaphragms with different configurations, including different types of nails, panel sheathings, among others. To address this purpose, 5 out of the 6 diaphragms experimentally tested – which are presented in Table 5 - were contrasted versus numerical models. Note that SL-OSB specimen was excluded from this comparison, because its loading protocol, as shown in Figure 3, produced notorious creep, mechanism which is not possible to reproduce by M-CASHEW [24]. Thus, this section considered monotonic analyses and one cyclic analysis (SL-PLY) with little to no creep. Loading set-up used in numerical models was to that used in experimental tests, i.e., the protocol suggested by ASTM E455 [23], applying the loads in the north-south direction.

The good agreement between experimental results and numerical models can be appreciated in Figure 8 and Table 5, which shows the comparison between global stiffness, peak capacity, ultimate displacement, and ductility. As previously mentioned, The IJ-OSB specimen showed an unexpected low stiffness, which was confirmed by its numerical model contrast, showing a clearly stiffer behavior within the linear range, although capacity and ductility appeared to be consistent with its corresponding experimental result.

The PLY/GWB specimens, i.e., those sheathed with gypsum over a plywood panel, were modeled only considering the plywood panel, since gypsum board did not appear to add any shear capacity. In this line, drywall screws were modeled directly as springs over plywood panels, attaching them to the framing underneath. These results have proven the feasibility of M-CASHEW to properly model light-frame diaphragms, as shown in Figure 8. It should be highlighted that the deformation of sheathing-to-framing connectors was the main flexibility source, while those attributable to framing were negligible [27].

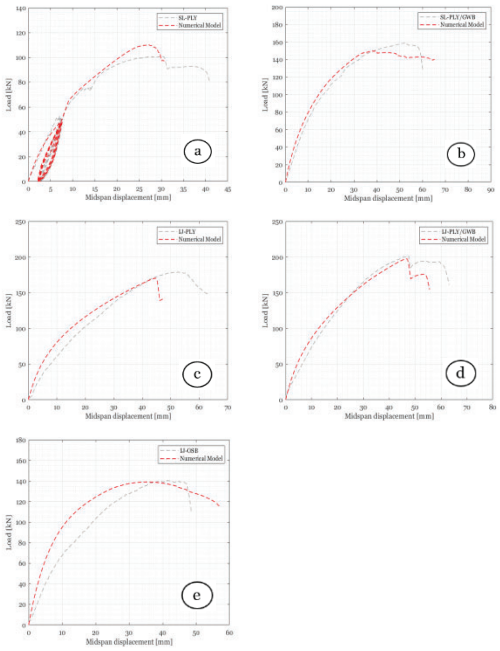

Figure 8: *Experimental and numerical model contrasts: (a)SL-PLY, (b) SL-PLY/GWB, (c) IJ-PLY, (d) IJ-PLY/GWB, I IJ-OSB.*

Table 5: *Structural properties of numerical models.*

Numerical model	F_0 kN	K_0 kN/mm	δ_u mm	μ -
SL – OSB	-	-	-	-
SL – PLY	110	9.8	30.7	2.1
	(1.1)	(1.05)	(0.74)	(0.56)
SL – PLY/GWB	150	8.67	65.2	4.5
	(0.93)	(1.15)	(1.08)	(1.43)
IJ – OSB	140	12.4	56.9	5.98
	(0.99)	(1.63)	(1.17)	(2.09)
IJ – PLY	170	8	47.6	3
	(0.95)	(0.68)	(0.75)	(1.27)
IJ – PLY/GWB	197	8.3	55.5	3.1
	(0.97)	(1.25)	(0.88)	(1.24)

https://doi.org/10.52202/069179-0447

(*) Values in parentheses correspond to the ratio between numerical and experimental results.

5 CONCLUSIONS

An experimental campaign was carried out on 8 full-scale industrialized timber diaphragms, proving its feasibility to withstand in plane shear loads without showing severe damage. The main conclusions of the present investigation are listed below:

Strength results resulted to be consistent with the recommendations provided by SDPWS [14], while experimental chord tension measurements suggest that an enlargement factor of 30% should be applied to chord tension obtained by mechanic principles. Anyway, more research on this topic must be performed to confirm such statement.

Experimental results showed that OSB-sheathed specimens were between 20-40% stiffer than those sheathed with plywood, regardless the framing. Also, I-Joist diaphragms results showed that those sheathed with 15.1 mm thickness plywood performed 27% stronger than those sheathed with 11.1 mm thickness OSB, consistent to Johansen's theory [34]. Likewise, I-Joist diaphragms developed larger peak capacities than sawn lumber diaphragms, which suggests that the more quantity of nails, the larger peak capacity, no matter if these nails have smaller diameters. Conversely, experimental results showed that sawn lumber diaphragms – sheathed with 2.9x65 mm nails - performed stiffer (between 10-70%) than their I-Joist counterparts – sheathed with 2.5x50 nails -. Thus, considering that I-Joist bare frame performed 100% stiffer than sawn lumber bare diaphragm, and that sawn lumber sheathed specimens contained less nail quantity than I-joist sheathed specimens, this leads to the conclusion that in plane stiffness is mainly controlled by nail diameter, while peak capacity is mainly controlled by nail quantity [27].

Peak capacity and in-plane stiffness were increased by using gypsum boards over plywood panels with 8x75 mm drywall screws. In fact, an increase of 15% was reached in the peak capacity, while a 20% improvement was noted in stiffness, particularly considering I-Joist specimens results.

Although the M-CASHEW [24] software had been mainly used to reproduce light-frame walls behavior until this research, with limited investigations attempting to predict diaphragm's structural response, this research proved the feasibility of M-CASHEW [24] to accurately predict mid-span displacements all the way to failure for different monotonically and cyclically loaded diaphragms. A more comprehensive discussion of these results is going to be available in literature soon.

Finally, these experimental results (which are deeply discussed in [27]) will serve as the basis for the inclusion of light-frame diaphragms in the Chilean regulation code [26]. Unit shear capacities, as well as the well-functioning behavior of mid-span displacement equations presented in here will experimentally support their adoption in the mentioned code.

REFERENCES

[1] Follesa, M., Fragiacomo, M., Casagrande, D., Tomasi, R., Piazza, M., Vassallo, D., Canetti, D., & Rossi, S. (2018). The new provisions for the seismic design of timber buildings in Europe. *Engineering Structures*, *168*, 736–747. https://doi.org/10.1016/j.engstruct.2018.04.090

[2] Fuentes, S., Fournely, E., & Bouchaïr, A. (2014). Experimental study of the in-plan stiffness of timber floor diaphragms. *European Journal of Environmental and Civil Engineering*, *18*(10), 1106–1117. https://doi.org/10.1080/19648189.2014.881760

[3] Dolce, M., Lorusso, V. D., & Masi, A. (1994). Seismic response of building structures with flexible inelastic diaphragm. *The Structural Design of Tall Buildings*, *3*(2), 87–106.

[4] ASCE. (2017). Minimum design loads and associated criteria for buildings and other structures. In *Minimum Design Loads and Associated Criteria for Buildings and Other Structures*. American Society of Civil Engineers (ASCE). https://doi.org/10.1061/9780784414248

[5] Bott, J. W. (2005). *Horizontal stiffness of wood diaphragms*. Virginia Tech.

[6] Countryman, D. (1952). Lateral tests on plywood sheathed diaphragms. *Douglas Fir Plywood Association (DFPA), Tacoma, WA*.

[7] Countryman, D., & Colbenson, P. (1954). *Horizontal plywood diaphragm tests: Laboratory Report No. 63*.

[8] Tissell, J. R. (1966). Horizontal Plywood Diaphragm Tests. *Laboratory Report*, *106*.

[9] Tissell, J. R., & Elliott, J. R. (1977). *Plywood diaphragms*.

[10] Zagajeski, S., Halvorsen, G. T., GangaRao, H. V. S., Luttrell, L. D., Jewell, R. B., Corda, D. N., & Roberts, J. D. (1984). Theoretical and experimental studies on timber diaphragms subject to earthquake loads. *Final Summary Report, Department of Civil Engineering, West Virginia University, Morgantown, WV*.

[11] Zhang, S., Daneshvar, H., & Chui, Y. H. (2021). Comparison of Lateral Load Performance of Light Wood Diaphragms Built with Sawn Lumber and Wood I-Joists. *Journal of Materials in Civil Engineering*, *33*(1). https://doi.org/10.1061/(asce)mt.1943-5533.0003544

[12] Waltz, N., & Dolan, J. D. (2010). I-Joist diaphragm systems: Performance Trends Observed with Full-Scale Testing. *Wood Design Focus*. www.dbmcontractors.com

[13] Yeh, B. J., Herzog, B., Skaggs, T., & others. (2016). Performance of full-scale I-joist diaphragms. *Proceedings of 3rd Meeting of International Network on Timber Engineering Research (INTER). INTER*, 15–49.

[14] American Wood Council. (2021). *Special Design Provisions for Wind and Seismic*. www.awc.org.

[15] Filiatrault, A., Christovasilis, I. P., Wanitkorkul, A., & van de Lindt, J. W. (2010). Experimental seismic

https://doi.org/10.52202/069179-0447

response of a full-scale light-frame wood building. *Journal of Structural Engineering*, *136*(3), 246–254.
[16] Mcmullin, K. M., Asce, M., & Merrick, D. S. (2007). *Seismic Damage Thresholds for Gypsum Wallboard Partition Walls*. https://doi.org/10.1061/ASCE1076-0431200713:122
[17] Mcmullin, K. M., & Merrick, D. (2001). *Seismic Performance of Gypsum Walls-Experimental Test Program Chapter 2. Literature Review*.
[18] Kirkham, W. J., Gupta, R., & Miller, T. H. (2015). Effects of Roof Pitch and Gypsum Ceilings on the Behavior of Wood Roof Diaphragms. *Journal of Performance of Constructed Facilities*, *29*(1). https://doi.org/10.1061/(asce)cf.1943-5509.0000490
[19] Walker, G., & Gonano, D. (1984). Experimental investigation of the diaphragm action of ceilings in resisting lateral loads on houses. *Proc., Pacific Timber Engineering Conf*, 543–550.
[20] Alsmarker, T. P. (1991). Structural diaphragms in wood-framed buildings. *Proc., Int. Timber Engineering Conf*, *4*, 4–354.
[21] Ministerio de Vivienda y Urbanismo. (2022). *Plan de Emergencia Habitacional 2022 - 2025*.
[22] Bari, N. A. A., Abdullah, N. A., Yusuff, R., Ismail, N., & Jaapar, A. (2012). Environmental Awareness and Benefits of Industrialized Building Systems (IBS). *Procedia - Social and Behavioral Sciences*, *50*, 392–404. https://doi.org/10.1016/j.sbspro.2012.08.044
[23] ASTM. (2019). ASTM E455-19: Standard Test Method for Static Load Testing of Framed Floor or Roof Diaphragm Constructions for Buildings. *ASTM International, West Conshohocken, PA 19428-2959*. https://doi.org/10.1520/E0455-19
[24] Pang, W., & Hassanzadeh Shirazi, S. M. (2013). Corotational Model for Cyclic Analysis of Light-Frame Wood Shear Walls and Diaphragms. *Journal of Structural Engineering*, *139*(8), 1303–1317. https://doi.org/10.1061/(asce)st.1943-541x.0000595
[25] Estrella, X., Guindos, P., Almazán, J. L., & Malek, S. (2020). Efficient nonlinear modeling of strong wood frame shear walls for mid-rise buildings. *Engineering Structures*, *215*. https://doi.org/10.1016/j.engstruct.2020.110670
[26] Instituto Nacional de Normalización. (2014). *NCh 1198. Madera - Construcciones en Madera - Cálculo*.
[27] Veliz, F., Estrella, X., Lagos, J., & Guindos, P. (2023). Testing and nonlinear modelling of industrialized light-frame timber diaphragms including optimized nailing and nonstructural sheathing. *Engineering Structures (under review)*.
[28] Grandmont, J.-F., Cloutier, A., Gendron, G., & Desjardins, R. (2010). *Wood I-joist model sensitivity to oriented strandboard web mechanical properties*.
[29] Folz, B., & Filiatrault, A. (2001). Cyclic analysis of wood shear walls. *Journal of Structural Engineering*, *127*(4), 433–441.
[30] Judd, J. P., & Fonseca, F. S. (2005). Analytical model for sheathing-to-framing connections in wood shear walls and diaphragms. *Journal of Structural Engineering*, *131*(2), 345–352.
[31] Jara, A., & Benedetti, F. (2017). *Informe No. 14 – Registro de estudio de ensayos de conectores*.
[32] Rizzi, E., Giongo, I., Ingham, J. M., & Dizhur, D. (2020). Testing and Modeling In-Plane Behavior of Retrofitted Timber Diaphragms. *Journal of Structural Engineering*, *146*(2). https://doi.org/10.1061/(asce)st.1943-541x.0002473
[33] ASTM. (2018). ASTM E2126-11: Standard test methods for cyclic (reversed) load test for shear resistance of vertical elements of the lateral force resisting systems for buildings. *ASTM International, West Conshohocken, PA: 2018.*
[34] Johansen, K. W. (1949). *Theory of Timber Connections*.